

行政院國家科學委員會專題研究計畫 期中進度報告

一維氧化鋅奈米結構的摻雜效應與光電特性研究(1/3)

計畫類別：整合型計畫

計畫編號：NSC94-2216-E-009-025-

執行期間：94年08月01日至95年07月31日

執行單位：國立交通大學材料科學與工程學系(所)

計畫主持人：陳三元

報告類型：精簡報告

處理方式：本計畫可公開查詢

中 華 民 國 95 年 5 月 27 日

一維氧化鋅奈米結構的摻雜效應與光電特性研究(1/3)

氧化鎂摻雜氧化鋅奈米柱之低溫製程與熱處理對於其結構與光電性質研究

Low-temperature process and effect of thermal annealing on structural and optical properties of MgO-coated ZnO nanorods

計畫編號：NSC94-2216-E-009-025-

執行時間：94/08/01 ~ 95/07/31

主持人：陳三元 教授

交通大學材料科學與工程學系

中文摘要

本研究利用化學溶液法在低溫環境中在氧化鋅薄膜的矽基板上，製備出規則排列氧化鎂摻雜的氧化鋅奈米柱，並分析氧化鋅奈米柱和氧化鎂包覆氧化鋅奈米柱後經熱處理後之結構及光學特性。氧化鋅奈米柱經過熱處理均可大幅增加光學品質，且在高溫下氧化鋅奈米柱的晶體結構也有明顯改變。氧化鎂包覆氧化鋅奈米柱後經熱處理後在化學特性分析中可以看出，鎂原子可以由氧化鋅奈米柱的缺陷路徑成功的擴散至奈米結構中，並且與鋅及氧元素產生化學鍵結反應。而在光學特性的研究上，氧化鋅奈米柱經過熱處理可改變可見光放射位置和強度，而且發現在紫外光放射有藍位現象，也證明鎂原子擴散至奈米結構，形成氧化鎂摻雜的氧化鋅奈米柱。經由本研究的結果顯示，我們可以利用常溫的水溶液合成法結合熱處理可以製備出規則排列氧化鎂摻雜的氧化鋅奈米柱。

關鍵字：陣列化 ZnO 奈米柱、氧化鎂包覆、熱處理、光電特性、微觀結構

Abstract

The effect of thermal annealing on the structural and optical properties of MgO-coated ZnO nanorods structures prepared by solution techniques were investigated with scanning electron microscopy (SEM), X-ray diffraction (XRD), and photoluminescence (PL) measurements. After thermal annealing process, Mg-doped ZnO nanorods have been grown on silicon substrates buffered with ZnO film. Structural analyses indicate that the nanorods grown on Si substrates are oriented in the c-axis direction and the nanorod possesses the single-crystalline hexagonal structure. No phase separation is observed when the annealing temperature increased to 900 °C. The MgO-coating ZnO nanorods annealed at above 800 °C showed the alloy formation due to diffusion of the Mg atoms into the ZnO nanorods. PL spectra displayed a blue shift of the near-band-edge emission, indicative of an increase in the band gap of the $Zn_{1-x}Mg_xO$ alloy.

Keywords: Alloyed ZnO nanorods ; MgO-coated ; Optoelectronic properties ; Thermal annealing ; Microstructure evolution

I. Introduction

ZnO has a wide band gap of 3.3 eV at room temperature, making it highly promising for great potential applications in manufacturing electronic and optoelectronic devices, especially ultraviolet (UV) laser devices [1]. Recent investigations have demonstrated that directionally grown ZnO nanorods can effectively reduce the threshold power, achieving UV lasing emission at room-temperature [2]. The photoluminescence (PL) spectra of ZnO typically exhibit UV and visible PL peaks. It is well-known that chemical doping, as well as intrinsic lattice defects, greatly influences electronic and optical properties of ZnO. Doped ZnO are of technological importance because of their great potential for applications to transparent conducting electrodes (doping group III B elements or fluorine) [3,4] and insulating or ferroelectric layers (doping Li or Mg)[5] in optoelectronic devices. Alloying ZnO phase with MgO or CdO has been investigated for widening the bandgap of the ZnO based materials [6]. According to the phase diagram of ZnO/MgO binary systems [7], the thermodynamic solid solubility of MgO in a ZnO matrix is less than 4 mol%. However, since the ionic radius of Mg^{2+} (0.57 Å) is almost the same as that of Zn^{2+} (0.60 Å) [8], Zn^{2+} can be replaced by Mg^{2+} in the ZnO matrix. Furthermore, it is well known that both physical characterization and optoelectronic properties are strongly influenced by the defect concentration in ZnO and this can be modified via thermal treatment under different atmospheres and annealing conditions.⁸ Therefore, it is important to investigate the effect of post-annealing on the microstructure and optical properties of MgO-coated ZnO nanorods. The variation of structural and optical properties of ZnO nanorods with thermal annealing was also discussed in this work for comparison.

2. Experimental

A ZnO buffered layer (with a thickness of around 100 nm) was deposited on Si substrate by radio frequency (rf) magnetron sputtering using 99.99% ZnO as the target. The ZnO nanorods were grown on the substrate. Then, the ZnO-coated Si substrates were placed in an equimolar (0.01M) aqueous solution of $Zn(NO_3)_2 \cdot 6H_2O$ and hexamethylenetetramine (HMT) at 75 °C for 10 h. Subsequently, the substrates were removed from the aqueous solutions, rinsed in distilled water, and dried overnight at room temperature. After grown, the ZnO nanorods were dispersed into $Mg(CH_3COO)_2$ aqueous solution. The solution was then stirred gently for about 30 min, at the same time, an aqueous solution of 0.03M Na_2CO_3 was dropped into the solution at the rate of $2.5 \text{ cm}^3 \text{ min}^{-1}$ and mixed for another 270 min. At the end it was washed with alcohol, then dried at 80 °C for 3 h, and fired at 300 °C for 0.5 h in Ar atmosphere. The coated nanorods were then immediately placed in a furnace preheated to 700 or 800 °C and annealed there for 5 or 30 min in air, O_2 , N_2 , or H_2/N_2 (5%/95%) atmospheres, followed by quenching. The obtained ZnO nanorods were characterized with scanning electron microscopy (JEOL-6500F). The crystal structure was elucidated using Siemens D5000 x-ray diffraction (XRD) with Cu $K\alpha$ radiation and a Ni filter. The chemical compositions were examined by

X-ray photoelectron spectroscopy (XPS) after the samples were first sputtered for 90 sec to remove the surface contamination by Ar ion. Photoluminescence of the ZnO nanorods were performed by the excitation from 325nm He-Cd laser at room temperature.

3. Results and discussion

3.1 Annealed uncoated ZnO nanorods

Figure 1 plots the room-temperature photoluminescence spectra of the ZnO nanorods annealed under various conditions. Only two emission peaks at 377nm (UV emission) and 595 nm (visible emission) were observed. It was found that UV emission intensities increase with annealing temperature, but the visible emission in post-annealed samples tends to disappear, suggesting that the native defects or non-radiative recombination can be reduced by post-annealing treatment in O₂ and N₂ atmospheres as shown in Fig. 1(a) and (b). However, the ZnO nanorods annealed in N₂ show stronger visible emission peaks compared to that annealed in oxygen atmosphere because the oxygen vacancies become the predominant point defects in N₂ atmosphere. In addition, a unique phenomenon was observed for the sample annealed in H₂/N₂ atmosphere, as presented in Fig. 1(c). An optimal UV emission occurs at the 600°C. It was believed that H₂/N₂ treatment is able to passivate native defects or impurities that contribute to visible transition, because the hydrogen atoms can be situated in various lattice positions. However, when the sample was exposed to H₂/N₂ at 800°C, the UV emission almost disappeared. This marked change can be attributed to the fact that a high-temperature reduction environment of H₂/N₂ could damage the crystal structure of the ZnO nanorods by surface etching [9]. Besides, it was also observed that the peak position of the longer-wavelength visible emission band shifts with different treatments. The peak position of the visible (deep-level) emission is related to the predominant defects in the ZnO nanorods and both defects of zinc interstitials and oxygen vacancies are strongly modified by changing annealing temperature and using different atmospheres. The relative PL ratios (I_{UV}/I_{DLE}) of the samples as a function of various atmospheres can be further summarized and presented in Fig. 1(d), revealing that the improvement in the optical quality of post-annealed ZnO nanorods is not only dominated by the annealing temperature but also the annealing atmosphere.

Figure 2(a) shows that the as-grown ZnO nanorods are perpendicular to the substrate with a uniform length of 900-950 nm. As annealed at 600°C in H₂/N₂, the cross-sectional morphology of the annealed ZnO nanorods is slightly different from that of the as-grown ZnO nanorods. It was found that the diameter of the annealed ZnO nanorods was locally necked. When the ZnO nanorods were annealed at 800°C in H₂/N₂, the surface image in Fig. 2(b) shows that all the ZnO nanorods were collapsed on the substrate, probably because of surface etching. These results may elucidate why the UV peak was rapidly and suddenly disappeared at 800°C in Fig. 1(c). In contrast, as the ZnO nanorods were annealed at 800°C in both O₂ and N₂ atmospheres, the morphology of the ZnO nanorods almost remain unchanged as compared

to that of the as-grown ZnO nanorods (Figs. 2(c) and 2(d)). However, at 1000°C in N₂ and O₂, the surface morphology of ZnO nanorods was changed from “rod-like” to irregular shape perhaps because of the melting and re-growth of the nanorods. As shown in Fig. 3(a), HR-TEM of the ZnO nanorods annealed at 1000°C in N₂ reveals that the ZnO nanorods were shortened to 300-400 nm, and became partially joined to their neighbors. The split diffraction spots in the central region of the SAED pattern suggest that the merged ZnO nanorods are not perfectly aligned in either the *a* (or *b*) and *c* directions, as presented in the inset of Fig. 3(b). Moreover, HR-TEM images of the ZnO nanorods in Fig. 3(c) demonstrate that partial amorphous was formed in the single-crystal ZnO nanorod. In addition, several lattice fringes (marked with arrows) appear in the edge of the ZnO nanorod in Fig. 3(d). Furthermore, according to X-ray photoelectron spectroscopy (XPS) analysis (not show here), the atomic ratio of O to Zn was approximately to 0.9 for the nanorods and the single of O²⁻ ions in the oxygen-deficient regions were almost covered by the background signal, this indicating these amorphous regions appeared to contain some structural defects. The primary defect type in the region may be considered as oxygen vacancies as evidenced by PL spectra.

3.2 Annealed MgO-coated nanorods

Fig. 4 shows the SEM images taken from several samples with highly uniform and densely packed arrays of MgO-coated ZnO nanorods grown on Si substrate. It can be observed that the surface of as-grown MgO-coated ZnO nanorods, as shown in Fig. 4(a), becomes rough. After annealed at 900°C in O₂ and N₂ atmospheres, Fig. 4(b) and 4(c) show the MgO-coated ZnO nanorods still kept hexagonal shape and the morphology of ZnO nanorods remained almost unchanged as compared to that of the as-grown ZnO nanorods [Fig. 2(a)]. However, as annealed at 800 °C in H₂/N₂, the cross-sectional morphology of the annealed ZnO nanorods in Fig. 4(d) is obviously different from that of the as-grown ZnO nanorods. Some of the ZnO nanorods annealed at 800°C in H₂/N₂ are slightly collapsed, probably because of surface etching.

Fig. 5 shows the X-ray diffraction (XRD) patterns of ZnO and Mg-doped ZnO nanorods annealed at 800°C and 900°C in H₂/N₂ and N₂(and O₂). All the XRD patterns indicate the formation of the wurtzite-type ZnO phase and the same (0 0 2) diffraction peak, implying that the Zn_{1-x}Mg_xO nanorods possess the same structure as that of the ZnO with preferentially orientation in *c*-axis direction. However, no diffraction peak of MgO crystal or Mg phase was detected in the XRD patterns, indicating that the Mg has been incorporated within the ZnO nanorods by means of substituting Zn.

It was postulated that some chemical bonding should exist between the oxide coating particles and the surface of ZnO nanorods, as illustrated in Fig. 6(a). The hydrogen bridges bonding and electrostatic forces played an important role in this process. [10]. On the other hand, part hydrolysis of ZnO nanorods surface was useful to the formation of the bonding.

During the process of hydrolysis, OH^- could react with Mg^{2+} , leading to MgO particles adhering better on the surface of ZnO nanorods.

As evidenced from high-resolution TEM (HRTEM) in Fig. 6(b), heterostructured core(ZnO)-shell(Mg.compound) nanorod were observed. The diameter of the core (ZnO nanorods) and the shell(MgO_x) thin layer is about 25 nm and 7 nm, respectively. Figure 6(c) shows that the {0002} lattice fringe of the ZnO nanorod core was parallel to the basal plane but no any lattice fringe can be identified in shell-MgO_x thin layer, indicating that the shell layer was amorphous. The EDS analysis in core region presents a strong ZnO signal and no Mg element. In contrast, in shell region, ZnO signal and Mg element were detected. The high-resolution TEM demonstrates that the ZnO nanorods were successfully coated with MgO_x layer.

Fig. 7 illustrates the room-temperature photoluminescence (PL) property of ZnO and Zn_{1-x}Mg_xO nanorods. The ultraviolet (UV) emission peak of ZnO is generally attributed to the exciton-related activity, and the deep level emission may be due to the transitions of native defects such as oxygen vacancies and zinc interstitials. A blue shift of the near-band-edge emission was observed when annealing temperature is above 700 °C. These results are in reasonable agreement with the thermal diffusion of Mg atoms at the MgO/ZnO heterointerface, which is observed only after annealing above 700 °C, [11] and with the formation of a Zn_{1-x}Mg_xO alloy. The UV emission peaks at 371 and 367 nm for the samples annealed at 800 and 900 °C, respectively, are attributed to the various Mg content in the Zn_{1-x}Mg_xO alloys formed at the different temperatures in O₂, N₂ and H₂/N₂, as presented in Fig. 7(a), (b) and (c), respectively. It can be found that the blue shift of UV emission seems independent of atmosphere but influenced by annealing temperature. However, a blue shift of the near-band-edge emission of H₂/N₂ annealing sample is not the same as that of O₂ and N₂ annealing sample, as shown in Fig. 7(d). Broadband visible emissions are observed in all PL spectra of the nanorods. It was noted that the visible emission from the annealed Zn_{1-x}Mg_xO nanorods at 800 °C in H₂/N₂ is centered at about 454 nm, providing the blue color. It may be related to the visible emission peak centered at 454 nm, indicating MgO diffusion process produces a new luminescent center in reduced atmosphere. In contrast, the visible emission peak of the ZnO nanorods annealed in H₂/N₂ is still at about 595 nm, [12] proving the visible emission peak centered at 454 nm has relation with MgO diffusion.) In contrast, the Zn_{1-x}Mg_xO nanorods annealed in O₂ or N₂ exhibits the orange emission centered at about 595 nm. However, visible emission from Zn_{1-x}Mg_xO nanorods annealed at 700 °C in H₂/N₂ seems to include two visible emissions which are centered at 454 and 595 nm. These results indicate that the MgO-coated ZnO nanorods have different luminescent centers in different annealing atmospheres.

Conclusion

The photoluminescence spectra indicate that the optical quality of the ZnO nanorods can be

changed and controlled by annealing the ZnO nanorods in various atmospheres at different temperatures. For the sample annealed in both O₂ and N₂ atmospheres, the room-temperature UV emission of the ZnO nanorods increases with the increase of temperature due to the reduction of structure defects. Structural analyses of Zn_{1-x}Mg_xO nanorods by XRD indicate that the hexagonal nanorods grown on Si substrates are oriented in the c-axis direction. As the MgO-coated ZnO nanorods were annealed at above 800 °C, the Zn_{1-x}Mg_xO alloy may be formed due to diffusion of the Mg atoms into the ZnO nanorods. A blue shift of the near-band-edge emission with increasing the annealing temperature was observed. It is noted that the visible emission from the Zn_{1-x}Mg_xO nanorods annealed at 800 °C in H₂/N₂ is centered at about 454 nm. In the contrast, the visible emission from the Zn_{1-x}Mg_xO nanorods annealed O₂ or N₂ is at 595 nm.

References

- [1] C. Weisbuch, H. Benisty, and R. J. Houdre, *J. Lumin.*, 85, 271 (2000).
- [2] M. H. Huang, S. Mao, H. Feick, H. Yan, Y. Wu, H. Kind, E. Weber, R. Russo, and P. Yang, *Science*, 292, 1897 (2001).
- [3] Minami, T.; Nanto, H.; Takata, S. *Jpn. J. Appl. Phys.* 23 (1984) L280.
- [4] Hu, J.; Gordon, R. G. *Sol. Cells*, 30 (1991) 437.
- [5] Joseph, M.; Tabata, H.; Kawai, T. *Appl. Phys. Lett.* 74 (1999) 2534.
- [6] T. Makno, Y. Sagawa, M. Kawasaki, A. Ohtomo, R. Shiroki, K. Tamura, T. Yasuda, H. Koinuma, *Appl. Phys. Lett.* 78 (2001) 1237.
- [7] S. Raghavan, J.P. Hajra, G.N.K. Iyengar, K.P. Abraham, *Thermochim. Acta* 189 (1991) 151.
- [8] R.D. Shannon, *Acta Crystallogr., Sect. A: Cryst. Phys., Diffr., Theor. Gen. Crystallogr.* 32 (1976) 751.
- [9] L. E. Greene, M. Law, J. Goldberger, F. Kim, J. C. Johnson, Y. Zhang, R. J. Saykall, and P. Yang, *Angew. Chem. Int. Ed.*, 42, 3031 (2003).
- [10] N. Arul Dhas, A. Zaban, A. Gedanken, *Chem. Mater.* 11 (1999) 806.
- [11] A. Ohtomo, R. Shiroki, I. Ohkubo, H. Koinuma, M. Kawasaki, *Appl. Phys. Lett.* 75 (1999) 4088.
- [12] C. C. Lin, H.-C. Liao, S. Y. Chen, and S. Y. Cheng. *J. Vac. Sci. Technol. B* 24 (2006) 304.

Acknowledgments

This work was financially supported by the National Science Council of the Republic of China, Taiwan under Contract No. NSC-94-2216-E-009-025.

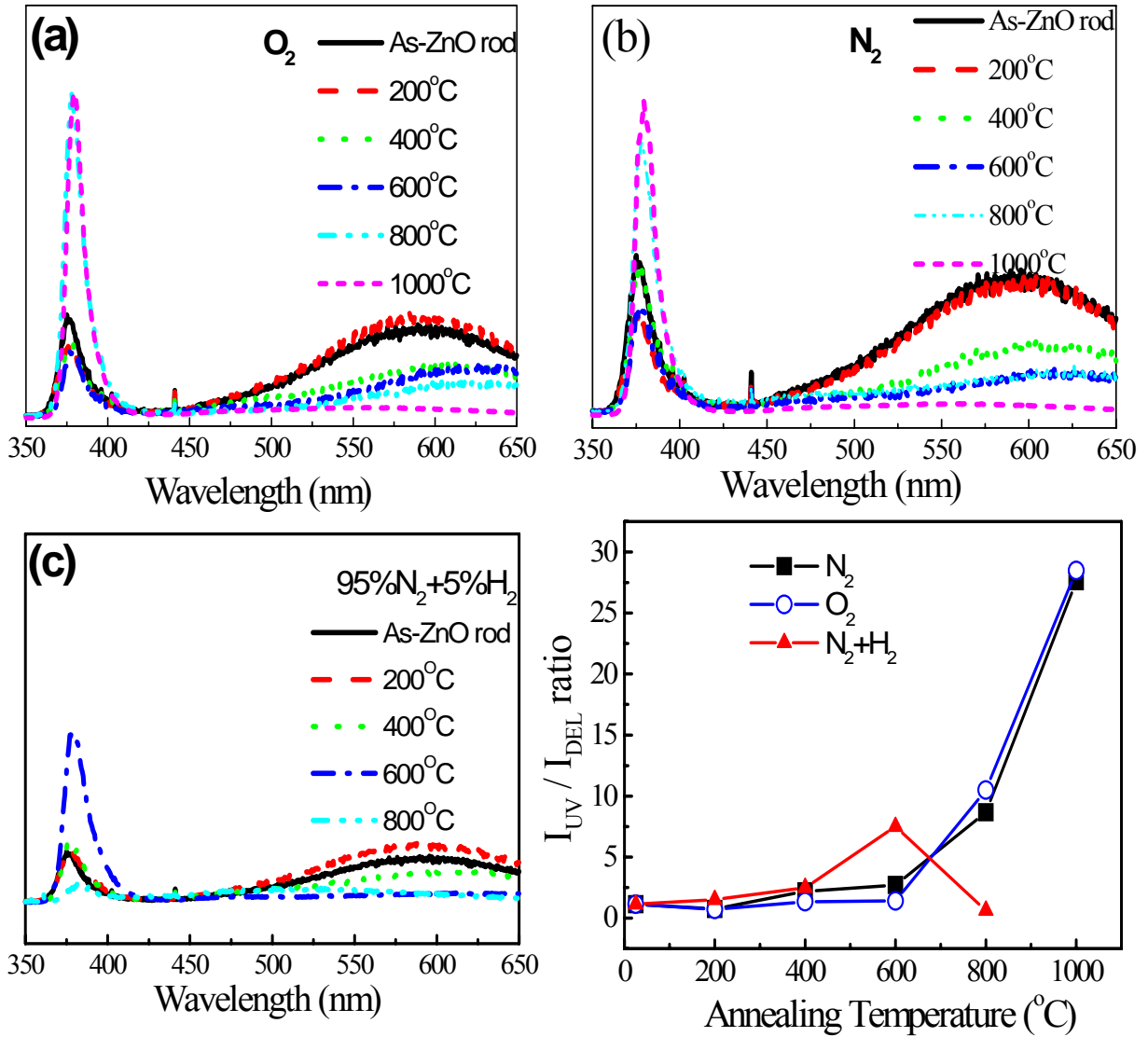


Fig. 1. Room-temperature PL spectra of ZnO nanorods annealed at various temperatures in (a) O_2 , (b) N_2 and (c) H_2/N_2 atmospheres. (d) I_{UV}/I_{DEL} of annealed ZnO nanorods dependent on various annealing conditions.

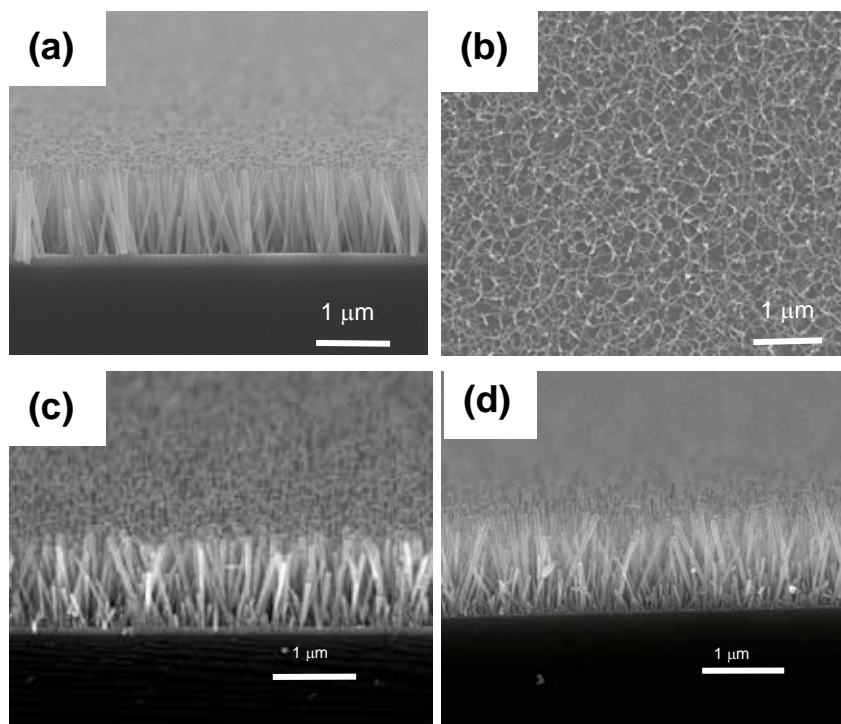


Fig. 2. SEM images of (a) as-grown ZnO and annealed ZnO nanorods at 800°C in (b) H₂/N₂. (c) O₂, and (d) N₂.

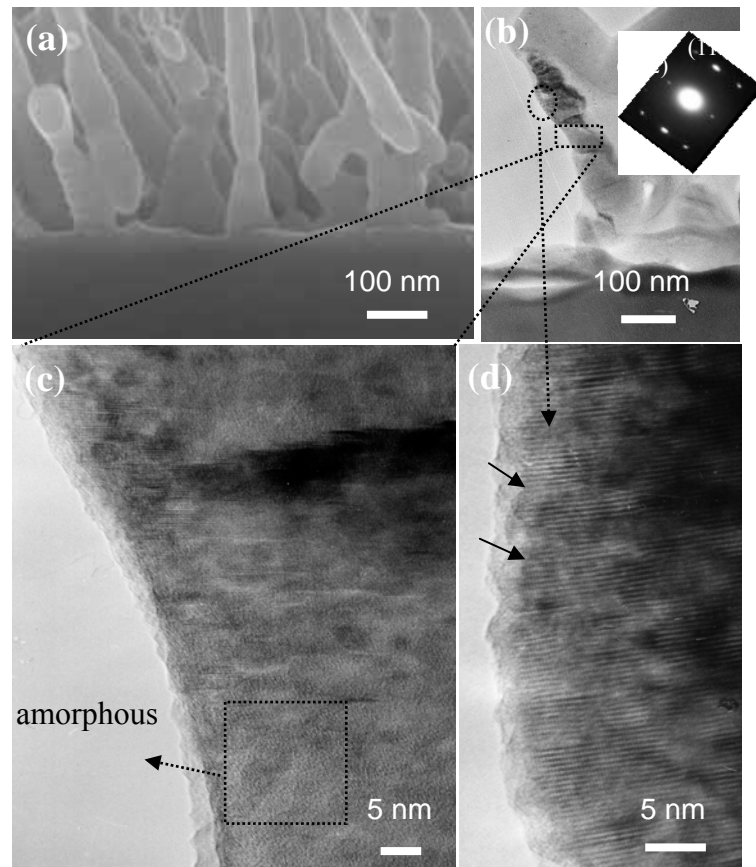


Fig. 3. (a) High-magnification SEM and (b) low-magnification TEM images of ZnO nanorods annealed at 1000°C in N₂ ambient with a corresponding diffraction pattern in the inset. A high-resolution TEM image of (b), showing the selected area in the (c) neck and (d) top of the ZnO nanorod.

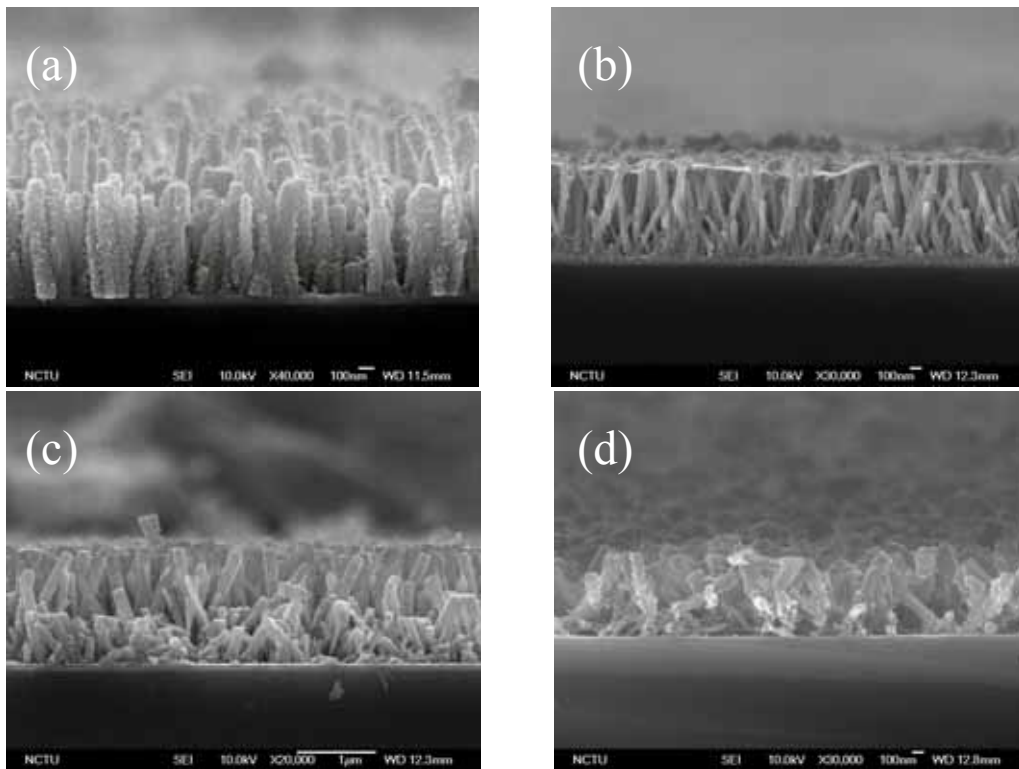


Fig.4 SEM images of (a) MgO-coated ZnO nanorods, and annealed at (b)900°C in N₂, (c) 900°C in O₂, and (d) 800°C in H₂/N₂.

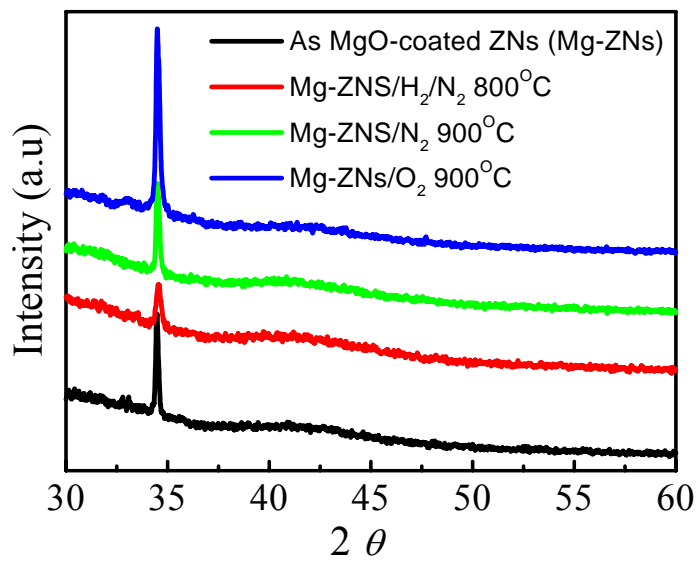


Fig. 5 XRD of MgO-coated ZnO nanorods annealed in various atmospheres.

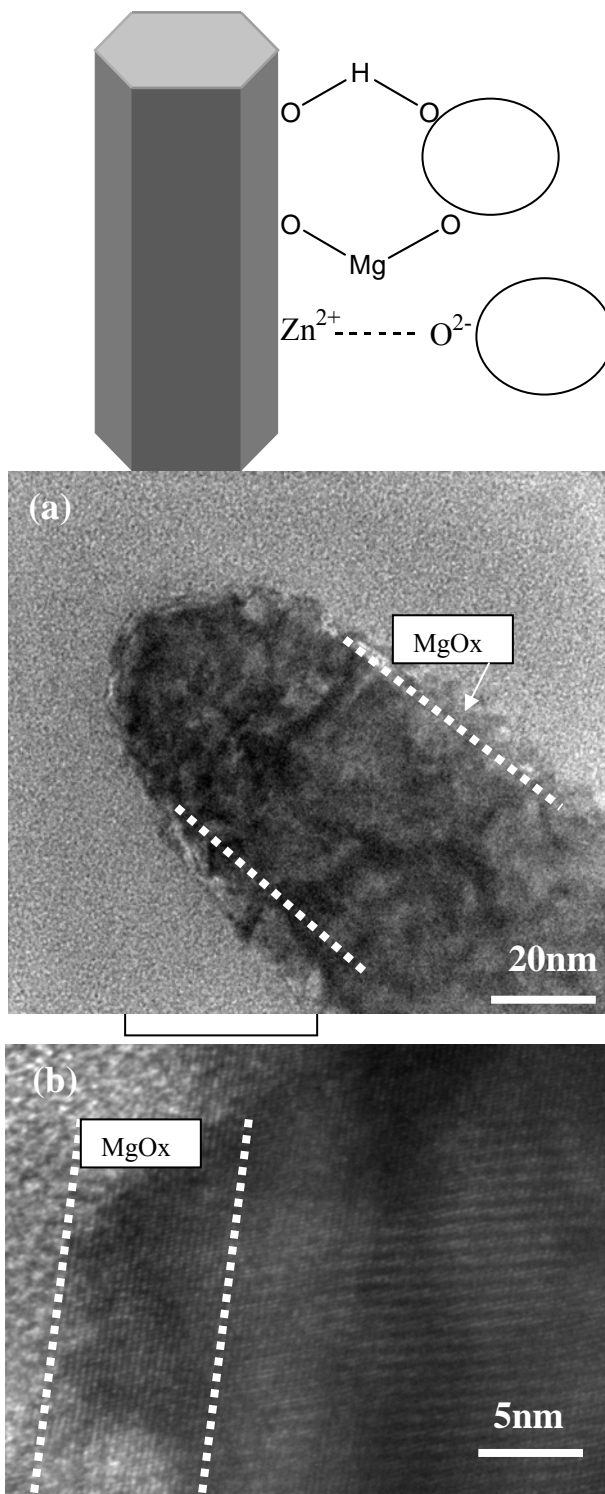


Fig. 6 (a) Model of bonding between MgO coating particles and surface of ZnO nanorods. (b) Low-magnification and (c) High-resolution TEM images of MgO-coated ZnO nanorod annealed at 800°C in O₂ atmosphere.

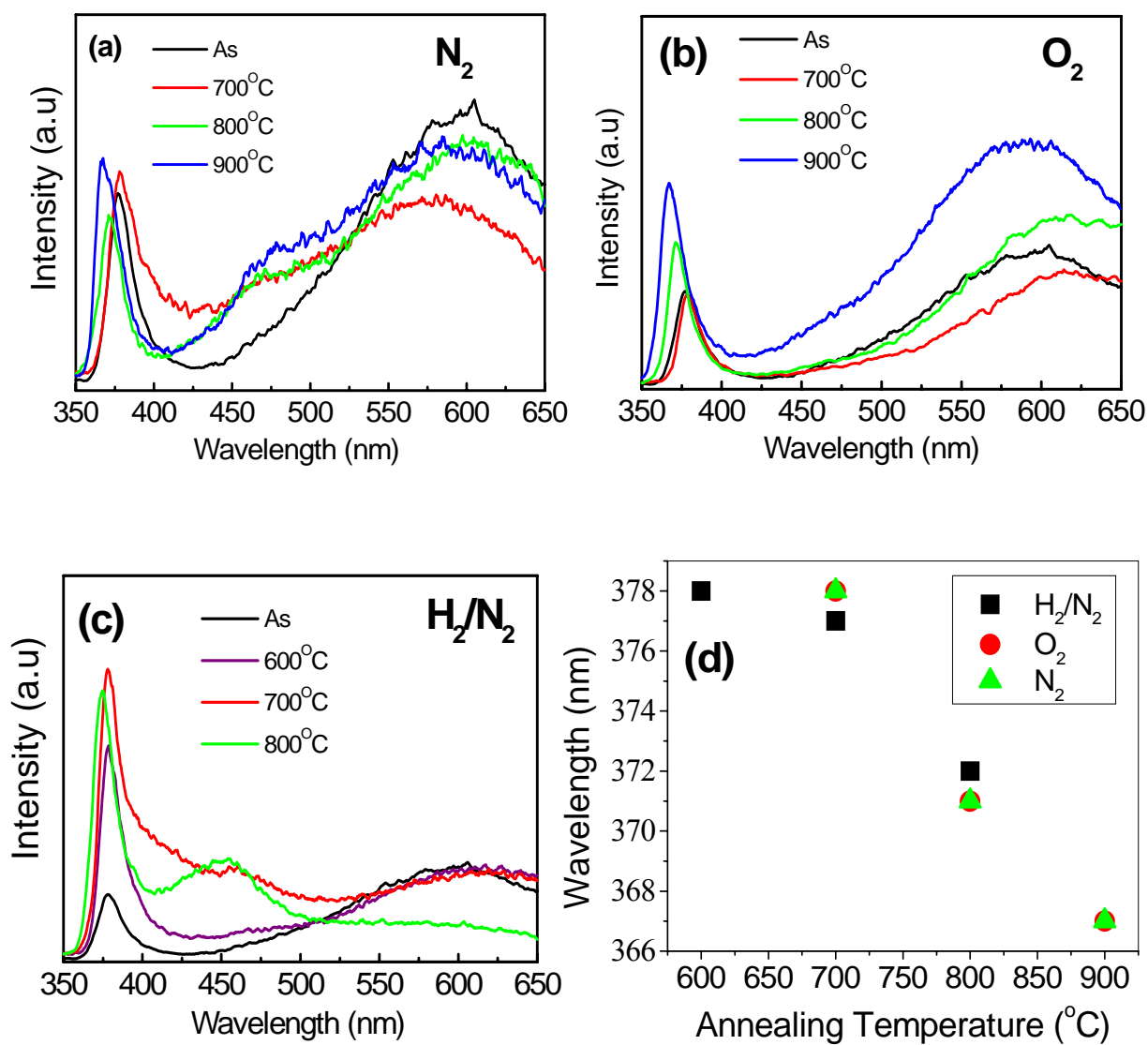


Fig 7. Room-temperature PL spectra of ZnO nanorods annealed at various temperatures in (a) N₂, (b) O₂, (c) H₂/N₂ atmospheres. (d) UV peak position of ZnO nanorods dependent on various annealing conditions